How Polymer Surface Diffusion Depends on Surface Coverage

Jiang Zhao

Joint Laboratory of Polymer Sciences and Materials, State Key Laboratory of Polymer Physics and Chemistry, Institute of Chemistry, Chinese Academy of Sciences, Beijing 100080, China

Steve Granick*

Departments of Materials Science and Engineering, of Chemistry, and of Physics, University of Illinois, Urbana, Illinois 61801

ABSTRACT: Measurements are presented of how surface diffusion of flexible polymers at the solid−liquid interface is controlled by surface coverage. Surface coverage is varied over the full range from dilute to saturated surface coverage. The method of measurement is fluorescence correlation spectroscopy (FCS), and the systems are poly(ethylene oxide) (PEG) and dextran adsorbed onto methyl-terminated self-assembled monolayers in buffered aqueous solution. A detailed study of PEG ($M_w = 10\,800$ g mol^{-1}) shows nonmonotonic behavior. The translational diffusion coefficient (D) at first increases with increasing surface concentration, presumably because the number of adsorption sites per molecule decreases as chains switch from pancake to loop−train−tail conformation. Excellent fits to behavior characteristic of a single diffusion process argue against aggregation or crystallization in the adsorbed state. In-situ ellipsometry measurements appear to rule out conformation changes to a hypothetical helical structure, as this would introduce birefringence to the adsorbed polymer layer causing deviations from the observed linear growth of apparent layer thickness with increasing surface coverage. For all three samples studied (PEG of $M_w = 10\,800$ and $20\,000$ g mol^{-1} and also dextran with $M_w = 10\,000$ g mol^{-1}), D at surface coverages larger than the estimated surface overlap concentration slow by 1 order of magnitude, presumably reflecting crowding and entanglement with neighboring chains.

Introduction

The goal to understand how the diffusion of polymer chains depends on polymer concentration comprised a large part of the agenda in polymer physics from the start. It seemed obvious to researchers, many years ago, that this and other aspects of dynamics at the level of individual molecules surely underpinned the macroscopic properties—viscoelasticity and adhesion, for example. Great names are associated with seminal understanding of the diffusion of flexible chains in the bulk—Rouse, Zimm, Doi, Edwards, and de Gennes on the theory side as well as, on the experimental side, important work by so many researchers that to single out individual names is not meaningful. Nowadays, study of the mechanisms and time scales of polymer diffusion in solution and in melts comprises a developed field of study, summarized in textbooks.[1−4] Interesting modern work does continue, for example, to understand diffusion in blends and microstructured block copolymers. Although one should never claim that understanding is definitive, polymer science has developed a rather mature understanding of how chain dynamics in bulk solution depend on chain length, chain architecture, and concentration.

The same is not so for polymer dynamics at surfaces. Ultrahigh-vacuum (UHV) surface science has studied surface diffusion for many years; polymer science has not. One basic limitation was that the needed experimental tools were not available. It is true that methods of dynamic light scattering have given insight into the global dynamics of polymer brushes.[5] It is also true that in the field of polymer adsorption work has approached this question from the perspective of understanding surface on−off (adsorption−desorption) kinetics. At the same time, it is also desirable to seek to understand in-plane polymer diffusion at surfaces, which is a distinctly different problem.[6−10]

Earlier reports from this laboratory considered the center-of-mass diffusion of adsorbed polymers in the limit of infinite dilution with special attention to the molecular weight dependence.[9,10] This left unanswered how polymer diffusion on a crowded surface differs from than in dilute situation. This is relevant because a long tradition of studying polymer diffusion in bulk (3D) solution considers the dilute situation to be the simplest and concentration dependence to present perturbations on this.[2,3] Here we consider the analogous question for polymers adsorbed at the solid−liquid interface. We present experiments that span the full concentration dependence of surface coverage, from dilute to saturated surface coverage.

This study, our initial effort in this direction, has the limitation that the systems we study are in aqueous solution, even though as concerns bulk diffusion, aqueous solutions are known to present potential complexity compared to the simpler case of nonpolar polymers in nonpolar solvents. The reason to choose aqueous media is simply that our method of in-situ diffusion measurement involves measuring fluorescence at the abundance of just a few dye molecules. The available fluorescent dyes, suited to this purpose, are best soluble in polar media.

Conformations of adsorbed chains lie at the heart of this matter. In this field of study, chains at the most dilute surface coverage are believed to adopt "pancake" conformations, flat against the surface, because general considerations show that the enthalpy gained outweighs the entropy lost.[4] At higher surface coverage it is not so; chains adopt fuzzy "loop−train−tail" conformations instead because sufficient chains are present to coat the surface with adsorbed segments without sacrificing so much conformational entropy.[4] We study two polymers: poly(ethylene glycol) (PEG) and dextran. A preliminary communication of a portion of this study was published previously.[11]

Experimental Section

Polymers. Poly(ethylene glycol) (PEG) terminated with an amino group at one end and a methoxyl group at the other end were purchased from Shearwater Polymer Inc. The number-average molecular weight was 10 800 g mol⁻¹, with the corresponding average degree of polymerization of 244, and the ratio of weight-average to number-average molecular weight determined by the manufacturer to be 1.02. A bright and photostable fluorescent dye, Alexa 488 (Molecular Probes), was attached at the terminal amino group. Dextran, a hydrophilic polysaccharide with a molecular weight of 10 000 g mol⁻¹ labeled with Rhodamine B, was also purchased from the same source.

For experimentation, PEG was dissolved in 1.0 mM phosphate buffer solution with pH = 8.4. Dextran was studied in deionized water (NANOpure II, Barnstead).

Surfaces. Methyl-terminated self-assembled monolayers on fused silica were adopted as the adsorption surface after preliminary experiments showed that when PEG adsorbed onto untreated fused silica, it diffused too slowly to be measured using our fluorescence measurement technique, FCS. Monolayers of hydrolyzed *n*-octadecyltriethoxysilane (OTE) were formed on fused silica cover slides (ESCO Products) using methods reported previously by this group.[12,13]

Ellipsometry. The thickness of adsorbed PEG was measured in situ using a home-built ellipsometer equipped with an electro-optical phase modulator, constructed after the Beaglehole design.[14] The signal-to-noise ratio was enhanced by conducting measurements at the Brewster angle. The measured ellipticity, $\rho \equiv \mathrm{Im}(r_p/r_s)$, served to quantify thickness of the adsorbed PEG. Here r_p and r_s are the reflectivity when polarization was parallel and perpendicular to the plane of incidence, respectively.

Fourier-Transformed Infrared Spectroscopy (FTIR). Infrared spectroscopy in the mode of attenuated total reflection (ATR) was used to determine the polymer surface coverage. Detailed descriptions of the experimental setup and procedure are described in earlier publications from this research group.[15,16] Briefly, a silicon crystal coated with an OTE monolayer was used as the substrate. Absorbance of the polymer methylene group was used to determine the quantity of polymer adsorbed (Γ).

Fluorescence Correlation Spectroscopy. A home-built apparatus for two-photon fluorescence correlation spectroscopy (FCS) was used to measure surface diffusion.[17,18] A detailed description can be found elsewhere.[19] Briefly, a mode-locked femtosecond pulsed laser providing <100 fs laser pulses served as the light source (Tsunami, Spectra-Physics). The laser beam was introduced into an inverted microscope (Axiovert S100 TV, Carl Zeiss) and tightly focused into the sample. Fluorescence excitation was achieved by two-photon excitation from 800 nm laser pulses. As a result, an excitation diameter of ~300 nm in the surface plane was created at the focal point of the objective lens. This dimension was calibrated from the diffusion of fluorescent dye molecules, fluorescein and Rhodamine 6G, in their aqueous solution and comparing the measured diffusion rates with literature values.

Fluorescence from the sample was collected by the same objective lens (PLAN-ACHROMAT 63X, oil-immersed, N.A. = 1.4), and the background light inside the signal was suppressed by a combination of a dichroic mirror and optical filters (ChromaTech). The fluorescence was then split into two parts with identical intensity and was detected separately by two photomultiplier tube (PMT)-based single photon counting modules (SPCM, Hamamatsu). The digitized outputs of the two SPCMs were collected by a FCS data acquisition board through its two input channels, and data analysis was conducted by its software (ISS).

In order to eliminate the possible artifact from the detector, for example the PMT after-pulsing process, cross-correlation was performed between the two channels. The diffusion coefficient and the average concentration of fluorescence molecules inside the excitation spot were obtained by fitting the experimental cross-correlation function to the expected results from a two-dimensional Brownian motion model.
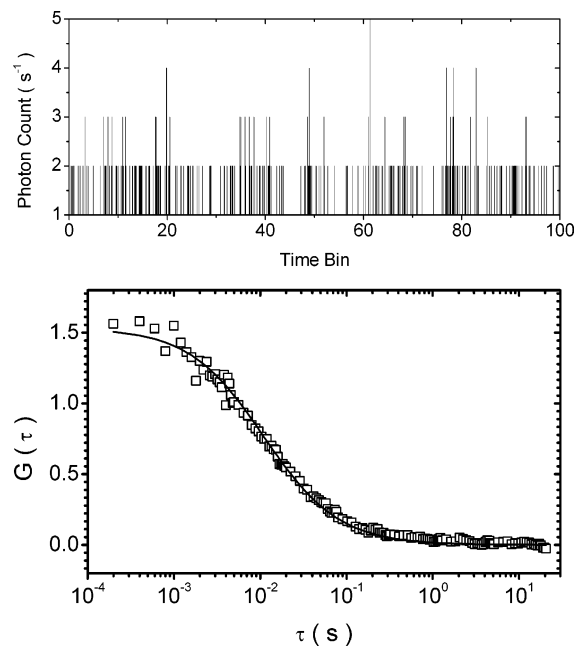

Figure 1. Illustrative temporal variation of fluorescence photon counts (top panel) and cross-correlation curve plotted against logarithmic time lag (bottom panel) for adsorbed dextran end-labeled with rhodamine B and diffusing on a hydrophobic surface. Line through the data is the fit to eq 1, the assumption of a single Fickian diffusion process. Based on this data and the calibrated diameter of the laser focus spot, the diffusion coefficient was 2.3 μm² s⁻¹ and the average concentration was 4 molecules μm⁻².

To begin the experiments, dye-labeled polymer was dissolved to the final concentration of roughly 1 nM. The polymer solution was exposed to the hydrophobic-modified silica surface, and about 5 min was allowed to allow polymer to adsorb. Then the sample was rinsed vigorously with solvent (phosphate buffer solution at pH = 8.4 for PEG and deionized water for dextran) to remove unattached polymer. After this process, FCS measurements were conducted.

In order to have a reliable measurement, it was important to have a precise focus. In these experiments, the focus of the laser beam was carefully adjusted onto the silica surface. During adjustments, the focal point was moved from the back solution toward the silica surface. Since the solution contained no labeled polymer, no noticeable fluorescence was detected there. As the focal point passed the surface containing adsorbed polymer, the fluorescence photon counts passed sharply through a maximum and subsequently dropped back to the level of dark counts, when the focal point moved into silica substrate. The position of highest fluorescence intensity corresponded to the surface position. Here, subsequent FCS measurements of polymer surface diffusion were conducted.

Results and Discussion

To illustrate, Figure 1 shows FCS data for diffusion of adsorbed dextran. In the top panel, the fluorescence photon count bursts show changes of fluorescence intensity from within the excitation spot as individual dextran molecules diffused into and out of the excitation area. The bottom panel shows the resulting cross-correlation function. Heuristically, it is useful to view this as setting the time scale of diffusion. As the spatial scale of diffusion is known from calibrating the diameter of the laser focus spot, the translational diffusion coefficient can be expected to scale as the square of this distance divided by the characteristic time. For quantification, the Gaussian intensity profile of laser excitation is also considered. By fitting the experimental data to the theoretical expectation for two-dimensional Brownian motion with a single diffusion Fickian diffusion coefficient, the diffusion coefficient and average
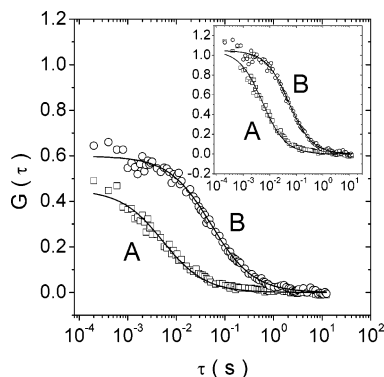
Figure 2. Cross-correlation function of PEG diffusing on a hydrophobic surface, plotted against logarithmic time lag. Curve A is for dilute surface coverage, 2.8×10^{-4} mg m^{-2}, which is less than the overlap concentration. The data imply $D = 5.0$ μm^2 s^{-1}. Curve B, for the crowded surface coverage (0.77 mg m^{-2}), implies $D = 0.4$ μm^2 s^{-1}. Inset: curves A and B after normalization to unity at short time. Lines through the data are the fit to eq 1, a single diffusion process.

concentration of fluorescent molecules were obtained. Specifically, the autocorrelation function for two-dimensional diffusion is known to be[9]

$$G(\tau) = \frac{1}{2\langle N \rangle}\left(1 + \frac{8D\tau}{w_0^2}\right)^{-1} \tag{1}$$

where D is the diffusion coefficient, N is the average number of molecules inside the laser spot, and w_0 is the diameter of the laser spot. Based on the data shown above, the diffusion coefficient of dextran in Figure 1 was 2.3 μm^2 s^{-1} and the average concentration was 4 molecules μm^{-2}.

The surface coverage was varied systematically. First, FCS measurements were performed at a very low concentration, and subsequently solutions of unlabeled polymers at higher solution concentration were exposed to the surface, thus raising the surface coverage while maintaining the low concentration of fluorescent-labeled polymer required by the principle of FCS measurement. By rinsing the sample vigorously with a solution of unlabeled polymer, the concentration of solution in the sample was believed to be homogeneous. Afterward, before initiating measurements of diffusion, the sample was allowed to stand 1−10 h to allow adsorption of unlabeled polymers to reach its equilibrium state.

Poly(ethylene glycol). Figure 2 illustrates two typical cross-correlation curves for PEG. Curve A concerns dilute surface concentration: about 16 molecules μm^{-2}, i.e., 2.8×10^{-4} mg m^{-2}, which is 245 $\times$ 245 nm^2 per molecule. This area per molecule is an order of magnitude larger than the size of a PEG molecule of two-dimensional configuration and corresponds unequivocally to less than the overlap concentration, c^*_{2D}. The diffusion of coefficient (D) is 5.0 μm^2 s^{-1}. In contrast, curve B is the cross-correlation curve of dye-labeled PEG immersed in unlabeled PEG molecules of the same molecular weight at the surface coverage of 0.77 mg m^{-2}. The time scale of the cross-correlation curve implies $D = 0.4$ μm^2 s^{-1}, much slower than the dilute case. Note that these measurements were obtained 1 h after adsorption, but control experiment showed that D did not change after 8−10 h of subsequent equilibration. This is consistent with the adsorption isotherm of PEG, which showed the equilibrium time for PEG adsorption to be about 40 min.

Figure 3 shows systematic measurements as a function of surface coverage. The diffusion coefficient first increased with increasing surface coverage, up to ~0.4 mg m^{-2}, and then dropped abruptly to a level an order of magnitude slower.
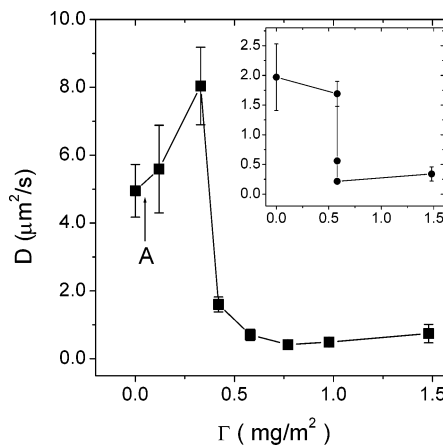

Figure 3. Surface diffusion coefficient of PEG ($M_w = 10\,000$ g mol^{-1}) plotted against surface concentration. Inset: same comparison but for PEG with $M_w = 20\,000$ g mol^{-1}. Error bars are the standard deviation of more than 20 measurements at different spots on the solid surface. Larger error bars at low surface coverage are believed to reflect heterogeneity from spot to spot on the solid surface. Lower error bars at high surface coverage are believed to reflect the fact that interactions with neighboring chains, rather than with the solid surface, are rate-limiting for translational diffusion. The estimated surface overlap concentration for pancake conformations, $c^*_{2D} \approx 0.05$ mg m^{-2}, is denoted in the figure by an arrow labeled "A".
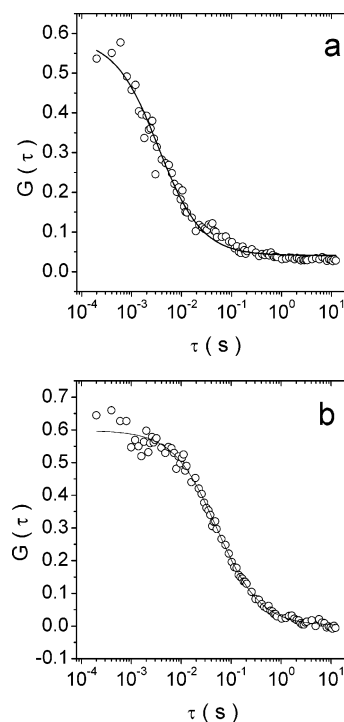

Figure 4. Representative cross-correlation functions plotted against time lag for PEG at dilute surface coverage (curve a) and at saturated surface coverage (curve b).

Similar measurements, displayed in the inset of Figure 3, were also performed using PEG of higher molecular weight, 20 000 g mol^{-1}. A similar change of diffusivity was observed.

What of possible artifacts? First, we considered the possibility of surface aggregation and crystallization. If these occurred, they would produce heterogeneous behavior and poor fits to the single-component diffusion presumed by eq 1; this was not observed. Figure 4 compares representative cross-correlation curves for dilute PEG and for PEG at high concentration, 0.77 mg m^{-2}. The former shows minor deviations from eq 1, as can be expected because it is unavoidable to have inhomogeneities
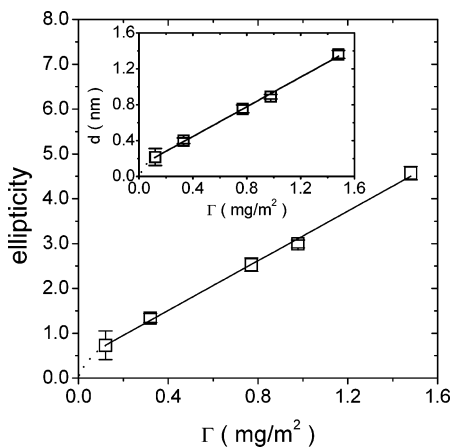
Figure 5. Elipticity and thickness (inset) of the PEG layer measured by in-situ ellipsometry. Thickness was calculated from the measured ellipticity by adopting a standard step layer model. The solid lines are the results of linear fitting.

in topography and surface chemistry, which control the rate of diffusion in this regime of dilute surface coverage. In contrast, the cross-correlation functions concerning diffusion at higher surface coverage agree better with eq 1. This implies that slower diffusion, observed in this situation, originated in interactions with neighboring PEG molecules that similarly were adsorbed. The latter rate-controlling situation resulted in a more homogeneous environment than when diffusion was rate-limited by interaction with the underlying solid surface itself. Excellent agreement of the data to expectations from a single diffusion process (eq 1) excludes the possibility of aggregation or crystallization of PEG.

Another conceivable issue was that adsorbed PEG might switch conformation from the random coil state, in solution, to helices at the surface. That PEG forms helices has been proposed in the literature.[20−22] To explore this hypothesis, ellipsometry measurements were conducted. Figure 5 shows ellipticity of adsorbed PEG as a function of surface concentration, and one observes that the dependence was linear, showing that the differential refractive index of adsorbed PEG remained constant as surface coverage increased. The calculated thickness of the adsorbed PEG layer as a function of the surface coverage is displayed in the inset of Figure 5. The calculation of the thickness was conducted on the basis of measured ellipticity. The detailed description of such a calculation can be found elsewhere.[23] This rules out the possibility of unusual conformation changes, as a hypothetical helical structure would have introduced birefringence to the adsorbed polymer layer, causing deviations from the observed linear dependence.

With these control experiments in mind, we attribute the dependence on surface coverage to different molecular conformations. To estimate the radius of gyration, we suppose by Occam's razor the same persistence length as for PEG molecules in bulk solution[7] and good solvent conditions on the surface just as in bulk solution. The two-dimensional radius of gyration of PEG (with molecular weight of 10 800 g mol^{-1}) is then estimated to be ∼13 nm, which is an order of magnitude smaller than the surface area per molecule in the most dilute state in Figure 3.

As surface coverage increased, eventually chains must overlap. At the overlap concentration, c^*_{2D}, the surface will be covered by a two-dimensional "pancake" of polymers. From the same calculation of molecular dimension as in the previous paragraph, $c^*_{2D} \approx 0.05$ mg m^{-2}. This is near the low end of Figure 3, as denoted by arrow A in this figure. Beyond c^*_{2D},
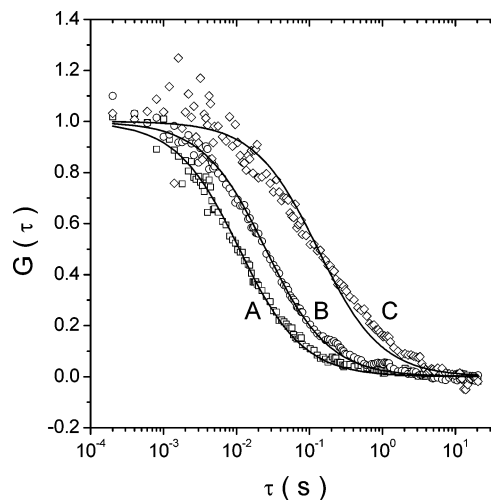

Figure 6. Normalized cross-correlation curves for adsorbed dextran. Curve A is for dilute surface concentration ($D = 2.0$ μm^2 s^{-1}). Curves B and C are for high concentration, 1.1 mg m^{-2} ($D = 0.2$ μm^2 s^{-1}). Curve B is for 1 h after adsorption of unlabeled dextran. Curve C is for 10 h of adsorption.

the molecules overlap and, as a result, repel one another if they remain in the flat pancake conformation. One possible consequence is that they undergo a conformational transition from pancake[4] to the "train−loop−tail"[1,6] conformation, in which only a fraction of potential adsorption sites meet the surface. It is reasonable to conclude that the drop of lateral mobility, at high surface coverage, stems from crowding. When the surface is crowded, the moving path of a given molecule is blocked by its neighboring molecules, and therefore, its motion is hindered. As imagined, each molecule needs to overcome multiple obstacles in order to accomplish lateral diffusion over distances that exceed the size of the molecule.

We note that the point at which sudden drop of diffusion was observed, 0.4 mg m^{-2}, is close to the two-dimensional melt concentration ($c_{2D,melt}$), measured from surface pressure measurements at the air−water interface.[24] At $c_{2D,melt}$, the interface is fully covered by polymer segments. Whether this is coincidence or has fundamental significance is unclear at this time. The suddenness of the change of the diffusion coefficient is phenomenologically reminiscent of "jamming" which has been much discussed in connection with three-dimensional systems,[25] but the analogy cannot strictly hold because decay of the fluorescence autocorrelation functions to zero show that these systems were ergodic. Recently, on the basis of molecular dynamics computer simulations, the alternative explanation was proposed that this point represents the transition from a monolayer to bilayer situation.[26] The observed slowing of D by an order of magnitude, at surface coverages larger than the estimated surface overlap concentration, presumably reflects crowding and entanglement with neighboring chains, but no mechanistic explanation is proposed at this time.

Dextran. Figure 6 shows illustrative cross-correlation functions for adsorbed dextran ($M_w = 10 000$ g mol^{-1}). At dilute surface coverage the cross-correlation function implies a diffusion coefficient of ∼2.0 μm^2 s^{-1}. At saturated surface coverage, the diffusion is slower by an order of magnitude, qualitatively like the case for PEG. But unlike PEG, in this system equilibration times come into play. In Figure 6, curves B and C show the cross-correlation function 1 and 10 h after subsequent adsorption of unlabeled dextran. Two features are clearly seen: first, the time scale is slowed by increasing the surface coverage, and second, the cross-correlation function after
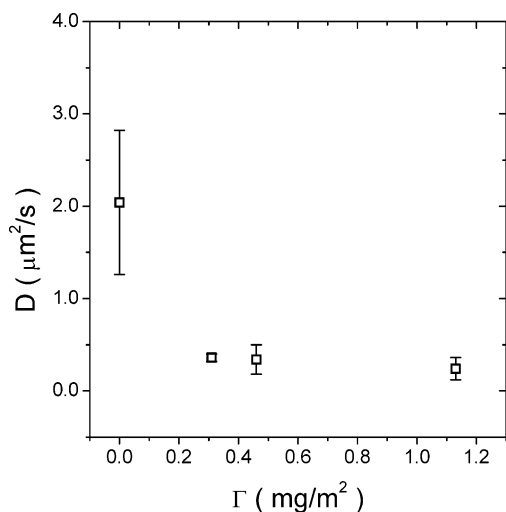
Figure 7. Surface diffusion coefficient of dextran as a function of the surface concentration. The diffusion coefficients plotted here refer to measurements after >10 h equilibration. Error bars are the standard deviation of ~20 measurements at different spots on the solid surface. The larger error bar at low surface coverage is believed to stem from heterogeneity from spot to spot on the solid surface. The lower error bars at high surface coverage are believed to reflect the fact that interactions with neighboring chains, rather than with the solid surface, are rate-limiting for translational diffusion.

10 h adsorption deviates more strongly from single-component fitting (eq 1) than that after 1 h adsorption. Figure 7 plots the diffusion coefficient, implied from fits to eq 1, vs surface coverage. The diffusion coefficients plotted here refer to measurements after >10 h equilibration. The diffusion coefficient exhibits a fast drop from 2.0 μm^2 s^{-1} at the most dilute concentration to 0.2 μm^2 s^{-1} at saturated concentration. For this sample, unfortunately the data as a function of surface coverage are more limited than for adsorbed PEG. Owing to polydispersity of this sample, we did not invest more effort to explore more carefully the dependence on surface coverage.

In order to understand the slow kinetics for dextran to equilibrate at the surface, the issue of the segmental sticking energy should be considered. Although we did not measure it, we think its sticking energy is similar to that of PEG ($\sim$0.5kT)[10] on the same surface because they have comparable surface mobility. The rigidity of chain may be the central factor. PEG is exceptionally flexible with the persistence length (l_p) of 3 Å,[9] whereas dextran is stiffer with l_p of 6 Å.[27] This may be relevant for understanding the slower equilibration that we observed for adsorbed dextran.

References and Notes

(1) Fleer, G. J.; Cohen Stuart, M. A.; Scheutjens, J. M. H. M.; Cosgrove, T.; Vincent, B. *Polymers at Interfaces*; Chapman and Hall: New York, 1993.
(2) Rubinstein, M.; Colby, R. H. *Polymer Physics*; Oxford University Press: New York, 2003.
(3) Doi, M.; Edwards, S. F. *Theory of Polymer Dynamics*; Clarendon Press: Oxford, 1986.
(4) de Gennes, P.-G. *Scaling Concepts in Polymer Physics*; Cornell University Press: Ithaca, NY, 1979.
(5) Fytas, G.; Anastasiadis, S. H.; Seghrouchni, R.; Vlassopoulos, D.; Li, J. B.; Factor, B. J.; Theobald, W.; Toprakcioglu, C. *Science* **1996**, *274*, 2041.
(6) Granick, S. *Eur. Phys. J. E* **2003**, *9*, 421.
(7) Maier, B.; Radler, J. O. *Phys. Rev. Lett.* **1999**, *82*, 1911.
(8) Maier, B.; Radler, J. O. *Macromolecules* **2000**, *33*, 7185.
(9) Sukhishvili, S. A.; Chen, Y.; Muller, J.; Schweizer, K.; Gratton, E.; Granick, S. *Nature (London)* **2000**, *406*, 146.
(10) Sukhishvili, S. A.; Chen, Y.; Muller, J.; Schweizer, K.; Gratton, E.; Granick, S. *Macromolecules* **2002**, *35*, 1776.
(11) Zhao, J.; Granick, S. *J. Am. Chem. Soc.* **2004**, *125*, 6242.
(12) Kessel, C. R.; Granick, S. *Langmuir* **1991**, *7*, 532.
(13) Peanasky, J.; Schneider, H. M.; Granick, S.; Kessel, C. R. *Langmuir* **1995**, *11*, 953.
(14) Mukhophadyay, A.; Law, B. M. *Phys. Rev. E* **2001**, *63*, 041605.
(15) Frantz, P.; Leonhard, D. C.; Granick, S. *Macromolecules* **1991**, *24*, 1868.
(16) Frantz, P.; Granick, S. *Macromolecules* **1994**, *27*, 2553.
(17) Magde, D.; Elson, E. L.; Webb, W. W. *Biopolymers* **1974**, *13*, 29.
(18) Berland, K. M.; So, P. T. C.; Gratton, E. *Biophys. J.* **1995**, *68*, 694.
(19) Zhao, J.; Bae, S. C.; Xie, F.; Granick, S. *Macromolecules* **2001**, *34*, 3123.
(20) Devanand, K.; Selser, J. C. *Nature (London)* **1990**, *343*, 739.
(21) Polverari, M.; Van der Ven, T. J. M. *J. Phys. Chem.* **1996**, *100*, 13687.
(22) Kunugasa, S.; Nakahara, H.; Fudagawa, N.; Koga, Y. *Macromolecules* **1994**, *27*, 6889.
(23) Law, B. M.; Mukhopadhyay, A.; Henderson, J. R.; Wang, J. Y. *Langmuir* **2003**, *19*, 8380.
(24) Kuzmenka, D. J.; Granick, S. *Macromolecules* **1988**, *21*, 779.
(25) Trappe, V.; Prasad, V.; Cipelletti, L.; Segre, P. N.; Weitz, D. A. *Nature (London)* **2001**, *411*, 772.
(26) Mukherji, D.; Müser, M. H. *Phys. Rev. E* **2006**, *74*, 010601(R).
(27) Rief, W.; Oesterhelt, F.; Heymann, B.; Gaub, H. E. *Science* **1997**, *275*, 1295.

MA062104L